*Int. J. Electrochem. Sci.*, 16 **(2021)** 210226, doi: 10.20964/2021.02.38

International Journal of
ELECTROCHEMICAL
SCIENCE
www.electrochemsci.org

# Electrospinning Synthesis of Ag Nanoparticles-doped Carbon Nanofibers for Voltammetric Determination of $H_2O_2$

*Yanqiong Zhu*[1,3], *Qinglan Miao*[2], *Baosan Han*[3,*]

[1] The Second People's Hospitial of Jingmen, Jingmen 448000, PR China
[2] College of Sciences, Shanghai University, Shanghai 200444, PR China
[3] Xinhua Hospital Affiliated to School of Medicine, Shanghai Jiaotong University, Shanghai 200092, China
[*]E-mail: hanbaosan@126.com

*Received:* 5 October 2020 / *Accepted:* 17 November 2020 / *Published:* 31 December 2020

Hydrogen peroxide ($H_2O_2$) has been widely used in various industries, including food production, pollution control, and textile bleaching. Therefore, it is necessary to determine its content for the sake of environmental and food safety. Silver nanoparticles (AgNPs) doped carbon nanofibers (CNFs) were prepared using electrospinning followed by calcination under a $N_2$ atmosphere as a novel electrocatalyst for the sensitive detection of $H_2O_2$. The composition, structure, and morphology of CNFs doped with AgNPs (AgCNFs) were characterized using Raman spectroscopy, X-ray diffraction, and scanning electron microscopy. The electrocatalytic activity of AgCNFs towards $H_2O_2$ reduction was evaluated using cyclic voltammetry and amperometry. As determined by electrochemical studies, the developed electrochemical sensor displayed a broad dynamic range of 0.01–50 mM and a detection limit of 3 μM ($S/N$ = 3).

**Keywords:** Electrospun; Ag nanoparticles doped carbon nanofibers; $H_2O_2$; voltammetry.

## 1. INTRODUCTION

Carbonaceous nanomaterials with different dimensions have been extensively employed in fields such as energy storage and conversion [1, 2], field emission displays [3, 4], theranostics [5, 6], and sensors [7, 8]. Carbon nanofibers (CNFs) and carbon nanotubes (CNTs) with one-dimensional structures have attracted significant interest because of their high aspect ratio of over a few hundreds, excellent mechanical properties and large surface area. Unlike CNTs, which are typically composed of concentric hollow graphene cylinders, the graphene layers in CNFs are not concentric and converge on the sidewalls, which increases the number of edge locations on the outer walls of CNFs and facilitates electron transfer of electroactive analytes [9, 10]. In addition, the functionalized surface area of CNFs

is higher than that of carbon nanotubes [11].

Electrospinning applies electrostatic force to draw charged threads of polymer solutions or polymer melts up to nanoscale fibers. In recent years, spinning carbon precursors is a popular method to fabricate CNFs, which are featured with tiny diameters, tremendous length, high specific surface area per unit mass [12]. Among the known spinning techniques, electrospinning has the advantages of low cost, simplicity, efficiency, and high yield in producing CNFs with diameters ranging from tens to several hundred nanometers [13–15].

Hydrogen peroxide ($H_2O_2$) has been extensively applied in various fields, including food production [16, 17], pollution control [18, 19], and textile bleaching [20, 21]. Several analytical techniques have been developed to detect $H_2O_2$ over the past several years including enzyme-based electrochemistry [22], fluorescence [17, 23], chemiluminescence [24] and spectrophotometry [25]. Compared to these techniques, non-enzymatic electrode-based electrochemical techniques are viewed as superior because of their simple equipment, low operating expenses, good sensitivity, low detection limits, and sound reliability [26–28].

Silver nanoparticles (AgNPs) have attracted increasing attention in metal-based nanomaterials because of their remarkable optical properties, excellent antibacterial activity, high catalytic activity, and strong surface-enhanced Raman effects [29, 30]. More importantly, AgNPs show good catalytic activity towards $H_2O_2$ reduction, which allows the design of non-enzymatic $H_2O_2$ sensors based on AgNPs [31, 32]. However, AgNPs tend to aggregate, which would significantly decrease their specific surface area. Accordingly, several AgNP hybrid materials have been prepared to minimize this limitation, including Ag-doped zeolitic imidazolate framework-8 nanoparticles [33], Ag-Au bimetallic nanomaterials [34], and AgNPs-reduced graphene oxide nanocomposites [35].

In this study, electrospinning and calcination were used to synthesize AgNP-doped CNFs (AgCNFs) for the electrochemical detection of $H_2O_2$. During the carbonization process, polyacrylonitrile (PAN) nanofibers were converted into CNFs, on which AgNPs were deposited. The temperature effect of the carbonization treatment on the morphology and structure of AgCNFs was investigated by SEM, XRD and Raman spectra. Furthermore, the analytical performances of AgCNFs modified glassy carbon electrodes (GCE) were studied in this work by various electrochemical techniques.

## 2. MATERIALS AND METHODS

### *2.1 Materials*

PAN (150,000 g $mol^{-1}$) was purchased from Aladdin Chemical Reagent Co., Ltd (China). N,N-dimethylformamide (DMF), $AgNO_3$, and $H_2O_2$ solution (30%) were bought from Sinopharm Chemical Reagent Co., Ltd (China). Milli-Q water was prepared and used throughout the test.

*2.2 Synthesis of* AgCNFs

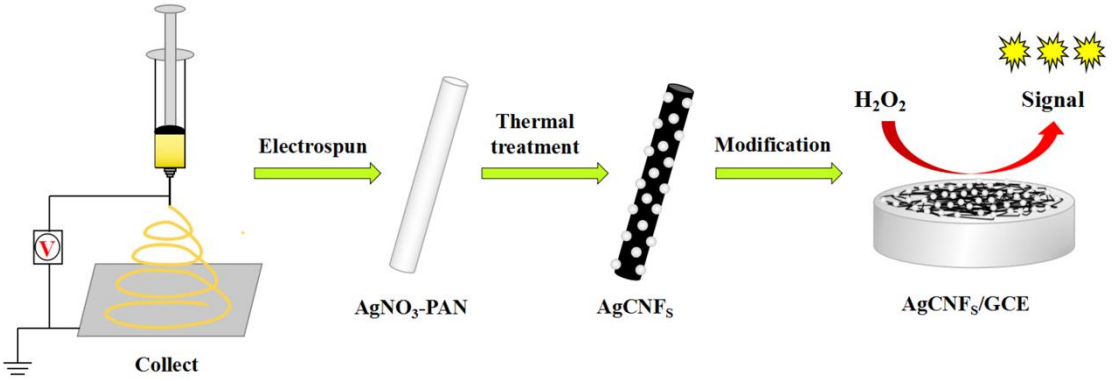


**Scheme 1.** The major steps for the synthesis of AgCNFs.

Scheme 1 shows the primary steps involved during preparation of AgCNFs. First, PAN was dissolved in a DMF solution (8 wt%) at 60 ℃ for 3 h with vigorous stirring to prepare the electrospun precursor. To this solution, 0.05 g $AgNO_3$ was added, and the solution was stirred overnight until a homogeneous solution was formed. Then, a homemade apparatus was used to perform the electrospinning. In brief, the electrospun solution was placed into a 10 mL syringe with a 0.5 mm-diameter stainless spinneret. The distance between the syringe needle and the metal collector was set to be ~15 cm, and a flow rate of 0.5 mL $h^{-1}$ was maintained during the test. A voltage of 15 kV was applied to the spinneret, which also served as an electrode. Subsequently, the electrospun fibers were allowed to dry for 12 h at 60 ℃, and then stabilized for 2 h at 280 ℃ in air. Afterwards, carbonization was performed at temperatures of 650 ℃, 750 ℃, and 850 ℃ respectively at an escalating rate of 3 ℃ $min^{-1}$ for 2 h under an $N_2$ flow.

*2.3 Apparatus and measurements*

The crystal forms of the prepared samples were investigated by X-ray diffraction (XRD, Rigaku DLMAX-2200, Japan) with Cu $K_\alpha$ radiation. Raman spectra were obtained using Raman microscope (Renishaw inVia, UK) with a 546 nm laser source. The morphology of the synthesized samples was identified by scanning electron microscope (SEM, JSM-6700F, Japan).

The electrochemical experiments including cyclic voltammetric and amperometric tests were performed at a CHI 842D electrochemical workstation in a three-electrode electrolyte cell. A bare GCEor AgCNFs modified GCE (GCE, Φ = 3 mm) was used as the working electrode. A saturated calomel electrode (SCE) and a Pt foil were used as the reference electrode and the counter electrode, respectively. All electrochemical experiments were performed at ambient temperature.

*2.4 Modification of electrodes*

Before surface modification, the GCE surface was cleaned with 0.05 μm alumina, washed

successively with water, ethanol and water, and then dried at room temperature. Afterwards, a homogeneous suspension was obtained by ultrasonically dispersing a certain amount of AgCNFs in 1 mL water. Finally, the suspension was dried under an infrared lamp after being dropped on the surface of the GCE.

## 3. RESULTS AND DISCUSSION

### *3.1 SEM analysis*

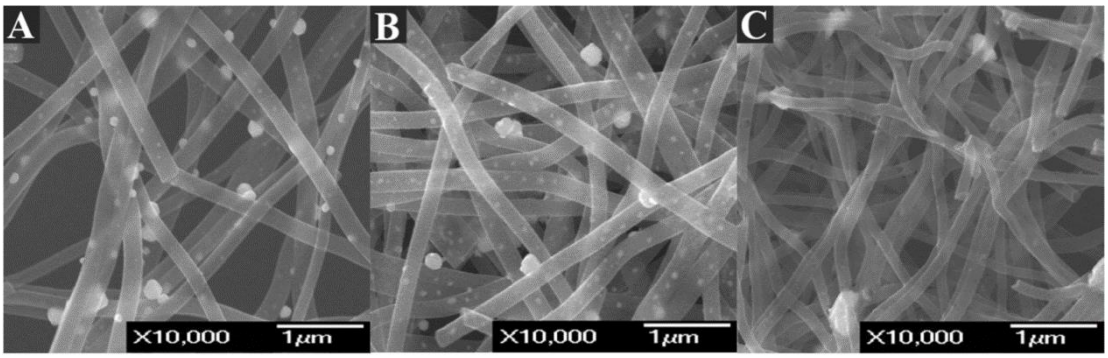


**Figure 1.** SEM images of AgCNFs carbonized at 650 ℃ (A), 750 ℃ (B) and 850 ℃ (C).

After carbonization in an $N_2$ atmosphere, CNFs were formed from PAN nanofibers, on which silver ions in the electrospun precursor were reduced to AgNPs. SEM was used to determine the effect of carbonization temperature on both the morphology and diameter of the polymer fibers. The SEM images of AgCNFs carbonized at 650 ℃ (AgCNFs-650, A), 750℃ (AgCNFs-750, B), and 850 ℃ (AgCNFs-850, C) are shown in Fig. 1. From these images, many large AgNPs can be observed on the surface of AgCNFs-650. When the temperature was increased to 750 ℃, the fiber diameter of AgCNFs-750 increased slightly. In addition, there are fewer large AgNPs on the surface of AgCNFs-750 compared to AgCNFs-650. The diameters of AgCNFs-750 are in the range of 200−350 nm, while AgNPs on AgCNFs-750 possess an average diameter near 70 nm. When the temperature was increased to 850 ℃, the diameter of AgCNFs-850 became smaller compared to that of AgCNFs-750, most likely due to the burn-off of the CNFs, which resulted in the aggregation of AgNPs and the subsequent detachment from the surface of AgCNFs-850.

### *3.2 XRD and Raman spectroscopy characterization*

Fig. 2A shows the XRD patterns of synthesized AgCNF-750. Five characteristic peaks at 38.1°, 44.4°, 64.4°, 77.4°, and 81.5°, are respectively indexed to (111), (200), (220), (311), and (222) faces of face-centered cubic (fcc) crystalline Ag, which are almost same as the values reported previously (JCPDS card No. 04−0783). Therefore, the XRD results support the claim that the silver ions were reduced to AgNPs by calcination.

The Raman spectra presented in Fig. 2B display bands at 1348 and 1586 $cm^{-1}$, which correspond to disordered (D) and graphitic (G) carbon phases at the three different carbonization temperatures. The D-band indicates that there are defects present in the graphite layer, while the original graphite features are associated with the G-band. In order to characterize the carbonization degree of CNFs, the relative intensity ratio of the D-band to the G-band (R-value) was evaluated. When smaller R-values are obtained, there is a higher amount of graphite clusters present in the sample. The relationship between the R-value and the domain size of the crystallite portion of graphite is denoted as La (nm) = 4.4/R. Herein, the R-value and La for AgCNFs-650, AgCNFs-750, and AgCNFs-850 were calculated to be (1.65, 2.67 nm), (1.19, 3.70 nm), and (1.06, 4.15 nm), respectively. These values indicate that increasing the carbonization temperature would improve the crystallite domain size of graphite on the CNF surface.

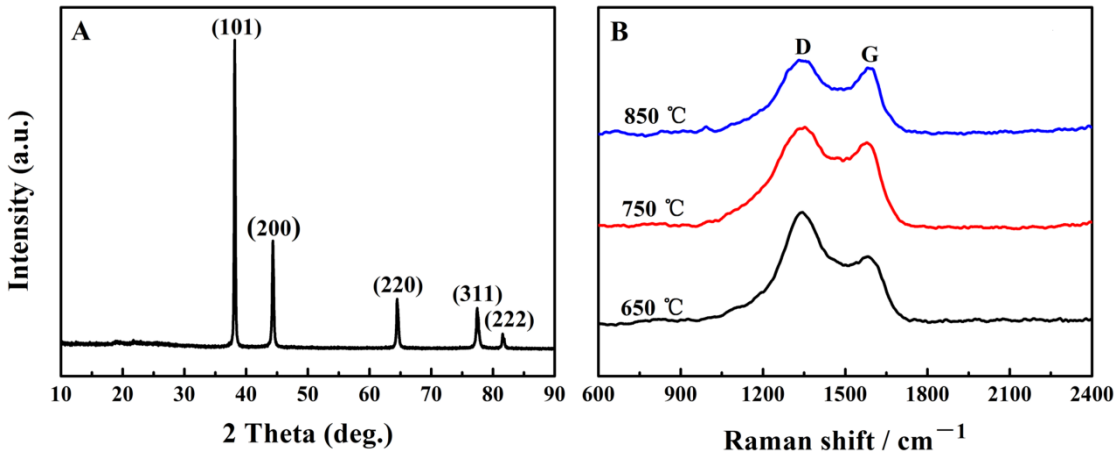


**Figure 2.** (A) XRD pattern of AgCNF-750; (B) Raman spectra of AgCNF-650, AgCNF-750 and AgCNF-850.

*3.3 Electrochemical behavior of AgCNFs/GCE*

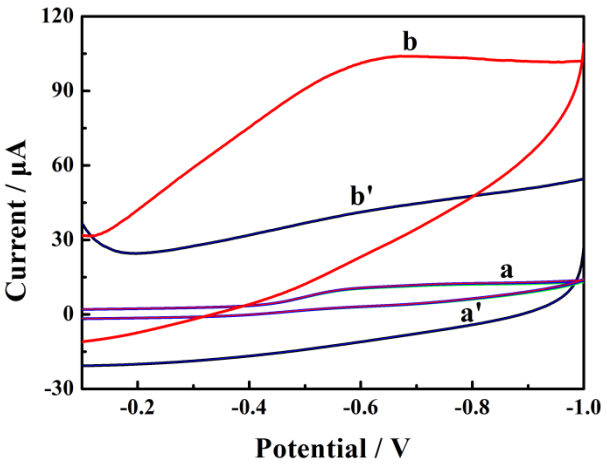


**Figure 3.** CVs of bare GCE and AgCNFs-750/GCE in the presence (a & b) and absence (a' & b') of 3 mM $H_2O_2$ in 0.1 M PBS (pH 7) at scan rate of 100 mV $s^{-1}$.

The electrocatalytic reduction of $H_2O_2$ at AgCNFs/GCE was studied by means of cyclic voltammetry (CV). CV behaviors of bare GCE and AgCNFs-750/GCE in the presence (a & b) and absence (a' & b') of 3 mM $H_2O_2$ in 0.1 M PBS at 100 mV/s are presented in Fig. 3. No evident reduction peak is displayed on the CV recorded on GCE (a') and AgCNFs-750/GCE (b'). After adding 3 mM $H_2O_2$ into 0.1 M PBS, no distinct CV peak is observed at bare GCE (a), while the current at AgCNFs-750/GCE (b) shows a remarkable increase. The electrochemical reaction mechanism can be described as follows [37, 38]:

$$H_2O_2 + e^- \rightarrow OH(ads) + OH^- \quad (1)$$

$$H_2O_2 + H^+ + OH(ads) + e^- \rightarrow 2OH(ads) + H_2O \quad (2)$$

The high specific surface area and electroconductivity of AgNPs and CNFs are responsible for their excellent electrocatalytic property.

### *3.4 Optimization of experimental parameters*

To obtain optimal electroanalytical performance, some parameters which may affect the current response of the developed electrochemical sensor were investigated including the amount of AgCNFs-750 on GCE, the pH of supporting electrolyte and the applied potential.

The amount of AgCNFs-750 on GCE is a key factor to influence the current response. Fig. 4A displays the electrocatalytic current of AgCNFs-750/GCE to 0.25 mM $H_2O_2$ at different concentration of AgCNFs (3−5 mg $mL^{-1}$) in 0.1 M PBS (pH 7.0). The current response enhanced as the concentration of AgCNFs-750 was increased from 3 to 4 mg $mL^{-1}$. Afterwards, the current response decreased at concentrations greater than 4 mg $mL^{-1}$. Hence, 4 mg $mL^{-1}$ AgCNFs-750 was selected to modify the electrode for amperometric $H_2O_2$ sensing.

The pH of supporting electrolyte has been optimized due to its influence on the current signal toward $H_2O_2$ reduction. The electrocatalytic current response in the range of pH 5−9 in 0.25 mM $H_2O_2$ is shown in Fig. 4B. At first, the response current rose as the pH was increased from 5 to 7. A maximum current was reached at pH 7, and then it decreased at pH values greater than 7. Therefore, a pH value of 7 was chosen for subsequent experiments.

The ameropmetric responses were also strongly influenced by the applied potential. Fig. 4C shows the electrocatalytic currents of 0.25 mM $H_2O_2$ within −0.4 ~ −0.8 V in 0.1 M PBS (pH 7.0). The current response was markedly amplified when the potential was increased from −0.4 V to −0.6 V. After that, the current response increased relatively slowly from −0.4 V to −0.8 V. Thus, the subsequent amperometric measurements were performed at −0.6 V.

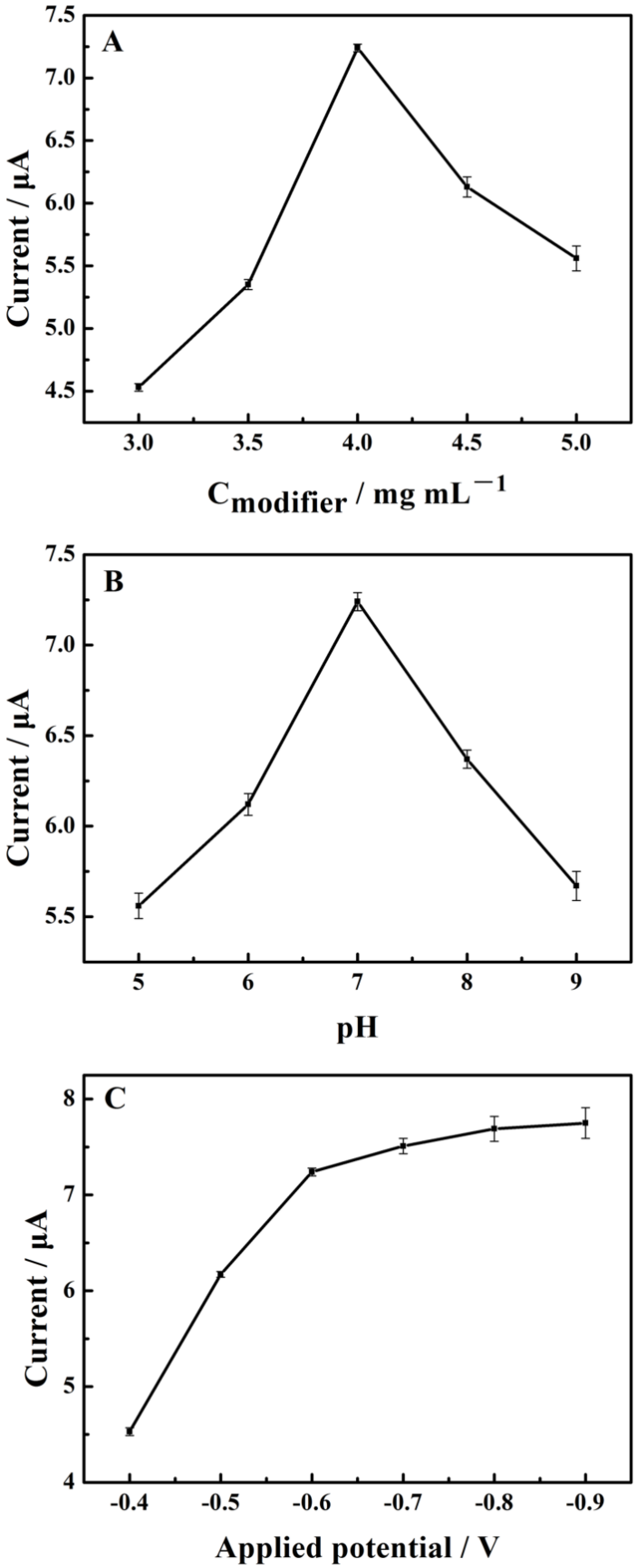


**Figure 4.** Effects of (A) the amount of modified AgCNFs-750 on GCE, (B) pH value and (C) applied potential on the amperometric response of 0.25 mM $H_2O_2$.

*3.5 Linearity, selectivity, reproducibility, and stability*

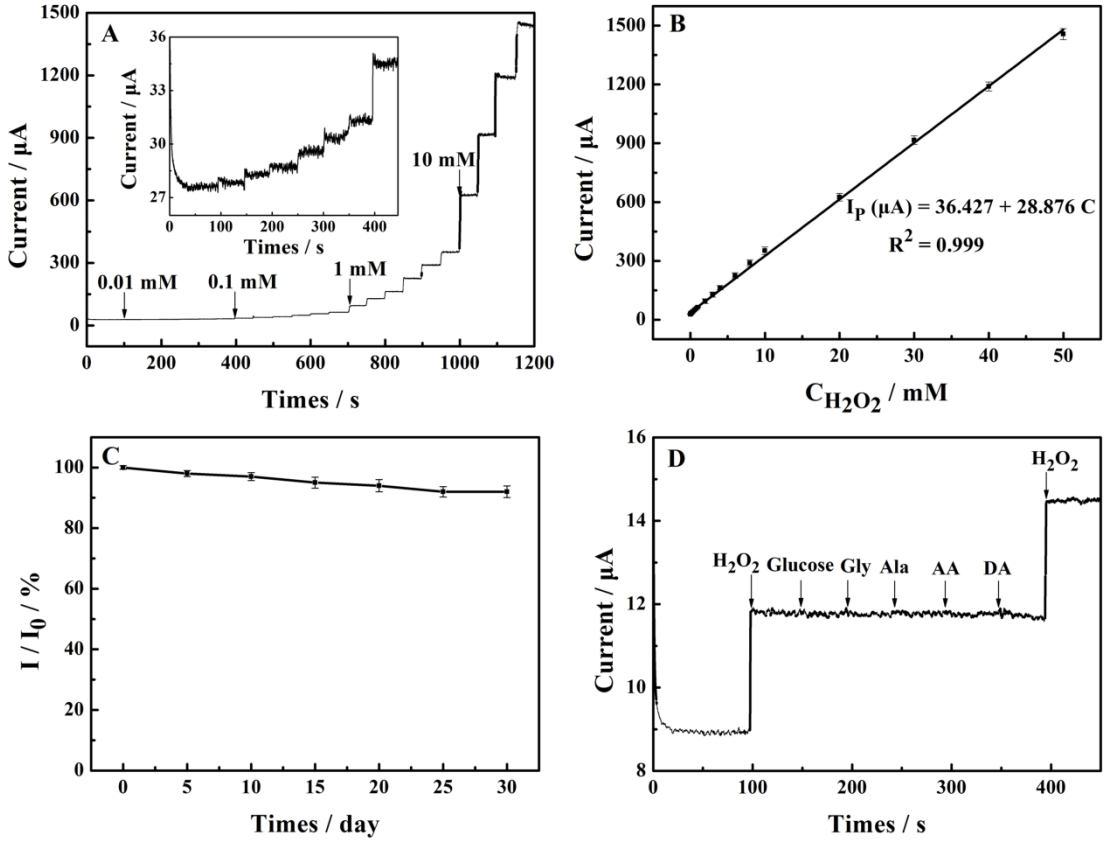


**Figure 5.** (A) Amperometric response of AgCNFs-750/GCE upon successive additions of different amount of $H_2O_2$ to 0.1 M PBS (pH 7) at –0.6 V and the inset shows the response for low concentrations; (B) The corresponding calibration curve; (C) The stability of AgCNFs-750/GCE; (D) Amperometric response of 0.1 mM $H_2O_2$, 1 mM glucose, 1 mM Gly, 1 mM Ala, 0.2 mM AA and 0.2 mM DA.

**Table 1.** Performance comparison of AgCNFs-750/GCE with other $H_2O_2$ sensors.

| Modified electrode | Linear range (mM) | Detection limit (μM) | Reference |
|---|---|---|---|
| AgNPLs-graphene | 0.02–1 | 3 | [29] |
| Roughed Ag | 0.01–22.5 | 6 | [39] |
| RuOHCF-MWCNT | 0.1–10 | 4 | [40] |
| AgNPs-MWCNT | 0.1–0.9 | 2.2 | [41] |
| AgNPs-(Ox-pTTBA)-MWCNT | 0.01–0.26 | 0.24 | [42] |
| CNF-PtNPs | 0.01–9.38 & 9.38–74.38 | 1.9 | [43] |
| Ag NPs-porous silicon | 0.002–0.5 | 0.45 | [44] |
| Fe-MOF/rGO | 0.005–0.945 | 0.5 | [45] |
| $MnO_2$-$Co_3O_4$ | 0.005–1.2 | 0.8 | [46] |
| Ag-$Fe_2O_3$/POM/rGO | 0.003–3 | 0.2 | [47] |
| AgNPs-CNFs | 0.01–50 | 3 | This work |

AgCNFs-750/GCE exhibits a rapid and stable response to $H_2O_2$ under the optimized conditions, as presented in Fig. 5A. A linear current response is observed when $H_2O_2$ concentration lies within the range of 0.01–50 mM, as shown in Fig. 5B. The corresponding regression equation can be expressed as: I (μA) = 36.423 + 28.876C (mM) ($R^2$ = 0.999) with a detection limit of 3 μM. Performance of the designed sensor is compared to those of the reported $H_2O_2$ sensors in Table 1 [29, 39–47]. From Table 1, metal/metal oxides such as roughed Ag, AgNPs, PtNPs, $Fe_2O_3$ and $MnO_2$-$Co_3O_4$, can be applied as non-enzymatic elctrocatalysts for $H_2O_2$ oxidation. In addition, carbon materials, including multi-walled carbon nanotube (MWCN), graphene and CNFs, could promote the electron transfer between the electrocatlysts and the substrate. The comparison shows that AgCNFs-750/GCE possesses a low detection limit as well as a wide linear range.

A biosensor should be able to selectively detect the targeting molecule from an interference environment. To examine the anti-interference response of AgCNFs-750/GCE, the possible interferents including glucose (10-fold), glycine (Gly, 10-fold), alanine (Ala, 10-fold), ascorbic acid (AA, 2-fold), and dopamine (DA, 2-fold) were added into $H_2O_2$ samples. Fig. 5C shows that glucose, Gly, Ala, DA, and AA did not obviously affect the performance of the biosensor, indicating the good anti-interference capability of the proposed biosensor toward $H_2O_2$.

The repeatability was evaluated by detecting a $H_2O_2$ sample with a modified electrode, which displays a relative standard deviation (RSD) of 4.3% over nine successive measurements. In addition, the stability of AgCNFs-750/GCE was also tested over a period of one month. The current response remains about 92.0% of its initial value. These results suggest that AgCNFs-750/GCE possess good repeatability and stability.

### *3.6 Real sample analysis*

The practical applicability of AgCNFs-750/GCE was tested by determining $H_2O_2$ in toothpaste. Briefly, 2.0 g toothpaste was mixed with 10 mL PBS (0.1 M, pH 7), and centrifuged prior to test, and the $H_2O_2$ concentration was determined using the standard addition method. Table 2 shows that AgCNFs-750 has the potential to detect $H_2O_2$ in real samples.

**Table 2.** Determination of $H_2O_2$ at AgCNFs-750/GCE in toothpaste samples (*n* = 3).

| Toothpaste samples | Added (mM) | Found (mM) | Recovery (%) | RSD (%) |
|---|---|---|---|---|
| 1 | 1 | 1.037 | 103.7 | 3.4 |
| 2 | 1 | 1.016 | 101.6 | 2.1 |
| 3 | 1 | 0.982 | 98.2 | 2.6 |

## 4. CONCLUSIONS

Electrospinning combining calcination was used to synthesize AgCNFs for the non-enzymatic detection of $H_2O_2$. Diverse morphologies were obtained by treating AgCNFs at three different

carbonization temperatures. After carbonization at 750 ℃, AgCNFs exhibited superior electrocatalytic activity towards $H_2O_2$ because of their high specific surface area and excellent electrical conductivities of AgNPs and CNFs. In addition, the proposed electrochemical sensor displays wide concentration range of 0.01–50 mM for $H_2O_2$ determination. The synthesized AgCNFs have provided a promising platform for the construction of CNFs-based sensors in the future.

STATEMENTS
The authors declare that there is no conflict of interest regarding the publication of this paper.

**References**


1. G.E. LeCroy, S. Yang, F. Yang, Y. Liu, K.A.S. Fernando, C.E. Bunker, Y. Hu, P.G. Luo and Y.P. Sun, *Coord. Chem. Rev.*, 320 (2016) 66.
2. M. Klose, R. Reinhold, K. Pinkert, M. Uhlemann, F. Wolke, J. Balach, T. Jaumann, U. Stoeck, J. Eckert and L. Giebeler, *Carbon*, 106 (2016) 306.
3. Y.C. Kim, S.H. Park, C.S. Lee, T.W. Chung, E. Cho, D.S. Chung and I.T. Han, *Carbon*, 91 (2015) 304.
4. K.J. Chung, N.W. Pu, M.J. Youh, Y. Liu, M.D. Ger, K. Cheng and J.C. Jiang, *Diamond Relat. Mater.*, 53 (2015) 1.
5. J. Ge, Q. Jia, W. Liu, L. Guo, Q. Liu, M. Lan, H. Zhang, X. Meng and P. Wang, *Adv. Mater*., 27 (2015) 4169.
6. Z.J. Zhang, J. Wang, X. Nie, T. Wen, Y.L. Ji, X.C. Wu, Y.L. Zhao and C.Y. Chen, *J. Am. Chem. Soc*., 136 (2014) 7317.
7. T.X. Zhu, Y.F. Zhang, L.Q Luo and X.L. Zhao, *ACS Appl. Mater. Interfaces*, 11 (2019) 10856.
8. Y. Chen, Y. Li, D.M. Deng, H.B. He, X.X. Yan, Z.X. Wang, C.H. Fan and L.Q. Luo, *Biosens. Bioelectron*., 102 (2018) 301.
9. V. Pillay, C. Dott, Y.E. Choonara, C. Tyagi, L. Tomar, P. Kumar, L.C. Du Toit and V.M.K. Ndesendo, *J. Nanomater*., 2013 (2013) 1.
10. W.E. Teo and S. Ramakrishna, *Compos. Sci. Technol.*, 69 (2009) 1804.
11. V. Vamvakaki, K. Tsagaraki and N. Chaniotakis, *Anal. Chem*., 78 (2006) 5538.
12. Z.Q. Su, J.W. Ding and G. Wei, *RSC Adv*., 4 (2014) 52598.
13. X.W. Mao, T.A Hatton and G.C. Rutledge, *Curr. Org. Chem*., 17 (2013) 1390.
14. S. Cavaliere, S. Subianto, I. Savych D.J. Jones and J. Roziere, *Energy Environ. Sci*., 4 (2011) 4761.
15. M.F. Zhang, X.N. Zhao, G.H. Zhang, G. Wei and Z.Q. Su, *J Mater Chem B*, 5 (2017) 1699.
16. C. L. Wagenaar and J. M. A. Snijders, *Int. J. Food Microbiol.*, 91 (2004) 205.
17. H. Julien, B. Benoit, S. Patrik, G. Vanessa, D. Julien and S. Jean-Manuel, *Food Chem.*, 211 (2016) 957.
18. H. Notsu, T. Tatsuma and A. Fujishima, *J. Electroanal. Chem*., 523 (2002) 86.
19. C. Shen, Y.J. Wang, J.H. Xu and G.S. Luo, *Green Chem.*, 18 (2016) 771.
20. S.I. Mistik and S.M. Yukseloglu, *Ultrasonics*., 43 (2005) 811.
21. C.H. Xu, X.X. Long, J.M. Du and S.H. Fu, *Carbohydr. Polym*., 92 (2013) 249.
22. L.Q. Luo, L.M. Zhu, Y.H. Xu, L.Y. Shen, X. Wang, Y.P. Ding, Q.X. Li and D.M. Deng, *Microchim. Acta*, 174 (2011) 55.
23. M. C. Y. Chang, A. Pralle, E. Y. Isacoff and C.J. Chang, *J. Am. Chem. Soc*., 126 (2004) 15392.
24. W.B. Shi, X.D. Zhang, S.H. He and Y.M. Huang, *Chem. Commun*., 47 (2011) 10785.
25. P. Nagaraja, J.S. Prakash, S.C. Asha, B.L. Bhaskara, S.A. Kumar, *Environ. Monit. Assess.*, 184 (2012) 5983.
26. L.L. Zhu, Y. Zhang, P.C. Xu, W.J. Wen, X.X. Li and J.Q. Xu, *Biosens. Bioelectron*., 80 (2016) 601.

27. L. Han, L. Tang, D.M. Deng, H.B. He, M. Zhou and L.Q. Luo, *Analyst*, 144 (2019) 685.
28. Y.Y. Li, L. Tang, D.M. Deng, Z.Y. Wu, J.H. Wang and L.Q. Luo, *Colloids Surf., B*, 179 (2019) 293.
29. L.J. Zhong, S.Y. Gan, X.G. Fu, F.H. Li, D.X. Han, L.P. Guo and L. Niu, *Electrochim. Acta*, 89 (2013) 222.
30. M. Zhou, L. Han, D.M. Deng, Z. Zhang, H.B. He, L. Zhang and L.Q Luo, *Sens. Actuators, B*, 291 (2019) 164.
31. S. Liu, J.Q. Tian, L. Wang, H.L. Li, Y.W. Zhang and X.P. Sun, *Macromolecules*, 43 (2010) 10078.
32. Y.H. Song, K. Cui, L. Wang and S.H. Chen, *Nanotechnology*, 20 (2009) 1.
33. A.S. Maybodi, S. Ghasemi and H.G. Rad, *Electrochim. Acta*, 163 (2015) 280.
34. W.Z. Li, L. Kuai, Q. Qin and B.Y. Geng, *J. Mater. Chem. A*, 1 (2013) 7111.
35. Q.Z. Li, X.Y. Qin, Y.L. Luo, W.B. Lu, G.H. Chang, A.M. Asiri, A.O. Al-Youbi and X. Sun, *Electrochim. Acta*, 83 (2012) 283.
36. D.L. Zhao, T.T. Wang, D. Han, C. Rusinek, A.J. Steckl and W.R. Heineman, *Anal. Chem.*, 87 (2015) 9315.
37. F.W. Campbell, S.R. Belding, R. Baron, L. Xiao and R.G. Compton, *J. Phys. Chem. C*, 113 (2009) 9053.
38. J.S. Easow and T. Selvaraju, *Electrochim. Acta*, 112 (2013) 648.
39. W.P. Lian, L. Wang, Y.H. Song, H.Z. Yuan, S.C. Zhao, P. Li and L.L. Chen, *Electrochim. Acta*, 54 (2009) 4334.
40. R.C. Pena, V.O. Silva, F.H. Quina and M. Bertotti, *J. Electroanal. Chem.*, 686 (2012) 1.
41. A.M. Yu, Q.X. Wang, J.W. Yong, P.J. Mahon, F. Malherbe, F. Wang, H.L. Zhang and J.M. Wang, *Electrochim. Acta*, 74 (2012) 111.
42. A. Abdelwahab and Y.B. Shim, *Sens. Actuators, B*, 201 (2014) 51.
43. Y. Li, M.F. Zhang, X.P. Zhang, G.H. Xie, Z.Q. Su and G. Wei, *Nanomaterials*, 5 (2015) 1891.
44. A.A. Ensafi, F. Rezaloo and B. Rezaei, *Sens. Actuators, B*, 231 (2016) 239.
45. S.L. Yang and N. Xia, *Int. J. Electrochem. Sci.*,14 (2019) 8.
46. S.J Li, Y. Xing, H. Y. Yang, J. Y. Huang, W.T. Wang and R.T. Liu, *Int. J. Electrochem. Sci.*,12 (2017) 6566.
47. N. Ross and N.C. Nqakala, *Anal. Lett.*, 53 (2020) 2445.